HHS Public Access

Author manuscript

Nat Commun. Author manuscript; available in PMC 2014 June 13.

Published in final edited form as:

Nat Commun. 2013 ; 4: 1952. doi:10.1038/ncomms2952.

Stac3 is a component of the excitation-contraction coupling machinery and mutated in Native American myopathy

Eric J. Horstick[1,*], **Jeremy W. Linsley**[2,*], **James J. Dowling**[3,*], **Michael A. Hauser**[4], **Kristin K. McDonald**[4], **Allison Ashley-Koch**[4], **Louis Saint-Amant**[1,5], **Akhila Satish**[1], **Wilson W. Cui**[2], **Weibin Zhou**[1,6], **Shawn M. Sprague**[1], **Demetra S. Stamm**[7], **Cynthia M. Powell**[8], **Marcy C. Speer**[9], **Clara Franzini-Armstrong**[10], **Hiromi Hirata**[11,#], and **John Y. Kuwada**[1,2,#]

[1]Department of Molecular, Cellular and Developmental Biology, University of Michigan, Ann Arbor, MI 48109, USA

[2]Cell and Molecular Biology Program, University of Michigan, Ann Arbor, MI 48109, USA

[3]Department of Pediatrics, University of Michigan Medical Center, Ann Arbor, MI 48109, USA

[4]Departments of Medicine and Ophthalmology, Duke University Medical Center, Durham, NC 27710, USA

[5]Departement de Pathologie et Biologie Cellulaire, Universite de Montreal, Montreal, Canada H3T 1J4

[6]Life Science Institute, University of Michigan, Ann Arbor, MI 48109, USA

[7]Department of Internal Medicine, University of California, Davis, Sacramento, CA 95817, USA

[8]Departments of Pediatrics and Genetics, The University of North Carolina at Chapel Hill, Chapel Hill, NC 27599, USA

[9]Center for Human Genetics, Duke University, Durham, NC 27710, USA

[10]Department of Cell and Developmental Biology, University of Pennsylvania School of Medicine, Philadelphia, PA 19104, USA

[11]National Institute of Genetics, Mishima 411-8540, Japan

[#]Correspondence should be addressed to: H.H. (hihirata@nig.ac.jp) or J.Y.K. (kuwada@umich.edu).
[*]These authors contributed equally to this work.

AUTHOR CONTRIBUTIONS

The zebrafish mutagenesis screen that isolated *stac3*^{mi34} was performed by L.S.-A., W.W.C., W.Z., S.M.S., H.H. and J.Y.K. The behavioral analysis of *stac3*^{mi34} was performed by H.H. and E.J.H. The electrophysiological and Ca^{2+} imaging analysis of *stac3*^{mi34} was performed by E.J.H. with some initial electrophysiological characterization by L.S.-A. Mutant rescue and NAM allele expression experiments were performed by E.J.H. Expression pattern of Stac3 was delineated by E.J.H. and H.H. Generation of anti-Stac3, immunoblots, co-immunoprecipitations, demonstration of maternal *stac3* transcript and Morpholino knockdown of Stac3 were performed by J.W.L. Meiotic mapping and molecular identification of *stac3*^{mi34} was performed by H.H. Electron microscopy was performed by C.F.-A. and J.J.D. Human *STAC3* was cloned by A.S. NAM clinical phenotyping, original pedigree analysis and biological sample collection were performed by C.M.P., D.S.S and M.C.S. Pedigree analysis of *STAC3* and Native American Myopathy was performed by J.J.D., K.K.M., A.A.-K. and M.A.H. The research was designed and the paper written by J.Y.K.

COMPETING INTERESTS STATEMENT

The authors declare that they have no competing financial interests.

Abstract

Excitation-contraction coupling, the process that regulates contractions by skeletal muscles, transduces changes in membrane voltage by activating release of Ca^{2+} from internal stores to initiate muscle contraction. Defects in EC coupling are associated with muscle diseases. Here we identify Stac3 as a novel component of the EC coupling machinery. Using a zebrafish genetic screen, we generate a locomotor mutation that is mapped to *stac3*. We provide electrophysiological, Ca^{2+} imaging, immunocytochemical and biochemical evidence that Stac3 participates in excitation-contraction coupling in muscles. Furthermore, we reveal that a mutation in human *STAC3* as the genetic basis of the debilitating Native American myopathy (NAM). Analysis of NAM *stac3* in zebrafish shows that the NAM mutation decreases excitation-contraction coupling. These findings enhance our understanding of both excitation-contraction coupling and the pathology of myopathies.

Introduction

Muscle contractions are initiated by depolarization of the voltage across the plasmamembrane resulting from synaptic release at the neuromuscular junction (NMJ). EC coupling is responsible for transducing the shift in the membrane voltage to increase cytosolic levels of Ca^{2+} that leads to contraction. Genetic defects in EC coupling components are associated with numerous congenital myopathies[1] that appear in infancy and are characterized by a variety of symptoms that include muscle weakness, difficulty with breathing and feeding, slower development, muscle cramps, stiffness, and spasm and in some cases susceptibility to malignant hyperthermia, which is an adverse reaction to general anesthesia that can be fatal. Despite the debilitating nature of congenital myopathies, their pathology is for the most part poorly understood. Congenital myopathies are highly heterogenous, and the genetic basis of many disorders are unknown.

In skeletal muscles EC coupling occurs at triads. Triads are junctions of the transverse tubules that are infoldings of the sarcomembrane and the sarcoplasmic reticulum (SR), an internal Ca^{2+} store. Changes in the membrane voltage of the transverse tubules are detected by the dihydropyridine receptor (DHPR), an L-type Ca^{2+} channel located in the transverse tubule membrane at triads[2–5]. DHPR is composed of the principal α1s subunit also called $Ca_V1.1$ that contains the pore and several accessory subunits. Activated DHPR, in turn, is thought to directly activate ryanodine receptor 1 (RyR1) Ca^{2+} release channels in the SR membrane side of the triadic junctions[6–9]. In mammalian skeletal muscles the DHPR also conducts extracellular Ca^{2+} to the cytosol but this is not required for EC coupling[10]. Interestingly in teleost skeletal muscles EC coupling is similarly independent of Ca^{2+} influx from the exterior and the DHPR appears to have evolved so that it no longer conducts Ca^{2+} [11]. Activation of RyR1 leads to release of Ca^{2+} from the SR to the cytosol and subsequently to contraction mediated by the contractile machinery.

EC coupling involves a complex of proteins localized to triads that include DHPR and RyR1. Although DHPR and RyR1 are well studied, the identity and roles of other components of the complex, how EC coupling is regulated and how the triadic molecular complex is established are poorly understood. Some of the other components of the triadic

complex include FKBP12, triadin, junctin and calsequestrin. Triadin, junctin and calsequestrin are SR proteins that regulate RyR1 from the luminal side of SR[12–14]. FKBP12 is an immunophilin, an immunosuppressive drug binding protein, that co-purifies and co-immunoprecipitates with RyR1 in striated muscles[15], and stabilize RyRs in their open state *in vitro*[16]. Two other cytosolic proteins that interact with EC components are SepN1 and calmodulin (CaM). SepN1 is a selenoprotein that co-immunoprecipitates with RyR1 and is associated with myopathy[17] and is required for formation of slow twitch muscles in zebrafish[18]. CaM can bind RyR and DHPR and modify EC coupling[19]. Despite the identification of these factors, the mechanisms for how they regulate EC coupling is poorly understood. These analyses illustrate the complexity of the EC coupling complex and its regulation, and suggest that a forward genetic strategy might be useful for identification of novel components for EC coupling.

Zebrafish have been useful for the analysis of a myriad of biological processes both because they are amenable to forward genetic screens and *in vivo* manipulations[20,21]. Pertinent to a genetic analysis of EC coupling, zebrafish muscles can also be analyzed *in vivo* with electrophysiology and live imaging[22,23]. We took advantage of these features to identify a zebrafish mutation in which EC coupling was defective. The gene responsible for the mutant phenotype encoded for Stac3, a putative muscle specific adaptor protein. Finally we found that a missense mutation in human *STAC3* is responsible for the debilitating, congenital Native American myopathy (NAM)[24,25].

Results

The *mi34* zebrafish mutant is defective in EC coupling

In order to identify new genes involved in the regulation of EC coupling, a forward genetic screen in the zebrafish was performed to isolate motor behavior mutants[26–30]. One mutation, *mi34*, was autosomal recessive with mutants dying as larvae and exhibiting defective motor behaviors at early stages of development. Normally zebrafish embryos exhibited spontaneous slow coiling of the body starting at 17 h postfertilization (hpf), touch-induced escape contractions of the body at 22 hpf and touch-induced swimming by 28 hpf[31]. Mutants were defective in all three motor behaviors with reduced amplitude of spontaneous coiling, decreased touch induced escape contractions and ineffective swimming (Supplementary Movies 1–6; Fig. 1a).

Aberrant behavior in mutants could be due to defects in the nervous system and/or skeletal muscles. If signaling within the nervous system were abnormal in mutants, then one would expect the output of motor neurons to muscles to be aberrant. To determine this, the synaptic response of muscles to tactile stimulation of the embryo was electrophysiologically recorded *in vivo*. Tactile stimulation initiated synaptic responses in both slow and fast twitch muscles in both wildtype sibling and mutant embryos. The evoked responses were comparable in amplitude, duration and frequency when measured with a low concentration of curare (see Methods) used to minimize muscle contraction (Fig. 1b; Supplementary Fig. S1). In order to see if the mutant muscles would generate action potentials in response to synaptic input, we examine muscle responses following sensory stimulation without curare which was possible because contraction by mutant muscles is minimal. These recordings showed that mutant

fast twitch muscles do respond with a burst of overshooting action potentials (Fig. 1c). Furthermore there were no obvious differences in the distribution of motor neuron terminals and muscle acetylcholine receptors (AChRs) between wildtype sibs and mutants when assayed with an antibody against SV2, a synaptic vesicle protein, and α-bungarotoxin that specifically binds AChRs (Supplementary Fig. S2). Thus the activity the nervous system and NMJ between wt and mutants are comparable and mutant muscles can initiate bursts of action potentials in response to synaptic input. Although we cannot rule of subtle changes, the severity of the behavioral phenotype is consistent with the mutation causing a defect in the muscle response to electrophysiological activation.

Activation of the NMJ leads to depolarization of the muscle membrane potential that in turn initiates muscle contraction. To examine how the mutation affects the relationship between muscle voltage and contraction, the membrane voltage of skeletal muscles were depolarized to various values and the amount muscles contracted was measured. Mutant muscles contracted much less than wildtype sib muscles at depolarized membrane potentials (Supplementary Fig. S3). The decreased contraction to depolarizations could be due to a defect in EC coupling or a defect in the contractile machinery. However, the fact that mutant and wildtype sib muscles contracted similarly when exposed to caffeine, an agonist of RyRs, (Supplementary Fig. S4) suggested that the contractile machinery was intact in mutants and that the store of Ca^{2+} in the SR was not grossly perturbed. Corroborating this finding, mutant muscles exhibited no obvious morphological defects early in development with apparent normal distribution of contractile proteins and other muscle proteins (Supplementary Fig. S4). Furthermore myofibers appeared normal in electron micrographs of larval skeletal muscles in *mi34* mutants (Fig. 2a). These findings pointed to a defect in EC coupling in mutant muscles.

The hallmark of EC coupling is the release of Ca^{2+} from the SR to the cytosol. EC coupling was directly examined *in vivo* by imaging Ca^{2+} transients in skeletal myofibers expressing the GCaMP3 Ca^{2+} indicator[32] during swimming. Swimming was evoked by application of NMDA, which activated the swimming network in the CNS[28]. Ca^{2+} transients were greatly reduced in both mutant slow and fast twitch fibers (Fig. 2b,c). Thus EC coupling in skeletal muscles was defective in the *mi34* mutants. Since EC coupling takes place at triads, reduced EC coupling in mutants could be due to abnormal formation of triads. However, longitudinal sections examined with TEM showed that there were triads at every intermyofibrillar junction with triads exhibiting comparable anatomy including two rows of feet in wtsib and mutant muscles (Fig. 2a). Although we cannot rule out a quantitative change in triadic anatomy, these data showed that the decrease in EC coupling in mutant muscles was not due to any obvious defect in triad anatomy.

stac3 is the basis for the *mi34* phenotype

A combination of meiotic mapping and analysis of zebrafish genome resources identified the gene responsible for the *mi34* phenotype as *stac3* (Supplementary Fig. S5; for details see Methods), a gene similar to murine *stac* that encodes an adaptor-like protein of unknown function[33]. *stac3* encodes for a putative 334 residue soluble protein with an N-terminal cysteine rich domain (CRD) similar to the C1 domain found in Ca-dependent protein kinase

and two SH3 domains (Fig. 3a). The mutant allele carried a point mutation that disrupted a splice donor site that led to the inclusion of intron 4 and a premature stop codon in the transcript. The mutation in *stac3* predicted a protein that was truncated within the N-terminal CRD suggesting that the *stac3*^{mi34} mutation was functionally null. Western blotting with an antibody generated against Stac3 that recognized a fragment of Stac3 consisting of the residues 1 to 63 (see Methods) revealed an approximately 49 kDa protein in wildtype embryos but no protein in mutants (Fig. 3b) suggesting that a truncated protein was not synthesized in mutants. *In situ* hybridization showed that skeletal muscles selectively expressed *stac3* during embryogenesis (Supplementary Fig. S6). Labeling with anti-Stac3 confirmed that Stac3 was specifically expressed by skeletal muscles and revealed that Stac3 co-localized with the DHPR$_{\alpha 1}$ and presumably RyR1 at muscle triads in wildtype but was not expressed in mutant embryos (Fig. 3c). These findings suggested that a mutation in *stac3* was responsible for defective EC coupling and that Stac3 was a component of the triadic molecular complex.

The molecular identity of the mutation was confirmed by mutant rescue experiments. Induced expression of *hsp70:stac3*^{wt}*-egfp* in mutant muscles rescued the behavioral phenotype and triadic localization of Stac3 whereas induced expression of *hsp70:stac3*^{mi34}*-egfp* did not (Fig. 4a). Furthermore Ca^{2+} imaging of mutant muscles co-expressing *stac3*^{wt}*-mCherry* and *GCaMP3* showed that wildtype Stac3 could restore Ca^{2+} muscle transients in mutant embryos (Fig. 4b,c). Given that Stac3 may be an adaptor protein and co-localizes with DHPR$_{\alpha 1}$ and RyR1, we examined whether Stac3 may be part of the triadic molecular complex. Indeed co-immunoprecipations with antibodies against pan-RyR and DHPR$_{\alpha 1}$ both pulled down Stac3 from wildtype adult muscles (Fig. 5) indicating that Stac3 is part of the DHPR/RyR1 complex found at triads. This was confirmed by generating a transgenic line of zebrafish (*α-actin:stac3*^{wt}*-egfp*) that expressed Stac3-EGFP in skeletal muscles and using anti-GFP to immunoprecipitate Stac3-EGFP from lysates of skeletal muscle of adult transgenic zebrafish. Mass spectrometry-based protein identification found that DHPR$_{\alpha 1s}$, DHPR$_{\alpha 2\delta 1}$, DHPR$_{\beta 1}$, RyR1 and RyR3 immunoprecipitated with Stac3-EGFP (Supplementary Table S1). Thus Stac3 is a component of the triadic complex that is required for EC coupling in skeletal muscles.

Although motor behaviors are greatly diminished in *stac3*^{mi34} mutants, they were not immotile. One possible reason for this might be the existence and action of Stac3 derived from maternally deposited *stac3* mRNA. In fact RT-PCR from 2hpf embryos (prior to zygotic expression[34]) found that *stac3* was maternally expressed (Fig. 6a). To see if the residual activity of skeletal muscles in *stac3*^{mi34} mutants was due to Stac3 translated from maternal mRNA, we knocked down Stac3 by injecting a translation blocking antisense Morpholino oligonucleotide (MO) against *stac3* message into embryos from crosses between heterozygous carriers. Anti-Stac3 labeling showed that *stac3* antisense MO injected embryos did not express Stac3 in skeletal muscles (Fig. 6b) confirming that the MO was effective. At 48 hpf wt embryos normally respond to tactile stimulation by swimming away. As expected from a cross between heterozygous carriers approximately 75% of the progeny injected with control MO responded to touch with swimming while 25% responded by slight muscle contractions (shivering) that failed to move the embryos effectively or were totally

immotile (Fig. 6c) indicative of the mutant phenotype. In antisense MO injected embryos, however, there was a significant increase in embryos that were either immotile or shivered and decrease in embryos that swam compared with control progeny. Significantly the proportion of immotile embryos increased from approximately 5% of control MO injected progeny to almost 40% of antisense MO injected progeny. Furthermore, the morphant phenotype was rescued by coinjecting an expression plasmid for *stac3*^{wt} along with the antisense MO demonstrating that the increased defective motility observed was not due to an off-target effect of the antisense MO, but rather a specific knockdown of maternal *stac3*. This suggests that elimination of both maternal and zygotic Stac3 results in immotility.

A mutation in human *STAC3* causes a congenital myopathy

The loss of Stac3 resulted in a progressive breakdown of myofibers during larval stages with apparent swollen SR observed by 7 dpf (Supplementary Fig. S7). Given the myopathic features of mutants we explored whether *stac3* mutations might cause congenital human myopathies. Human *STAC3* mapped to chromosome 12q13–14, and its specific location was within the previously defined genetic locus for the congenital Native American myopathy (NAM)[24,25]. NAM is an autosomal recessive disorder found within the Lumbee Native American population of North Carolina that was characterized by a constellation of clinical features including congenital onset of muscle weakness, susceptibility to malignant hyperthermia, multiple joint contractures and dysmorphic facial features including ptosis. Patient muscle biopsies revealed a non-specific myopathic pattern. Furthermore, 36% of afflicted individuals die by the age of 18. The genetic basis of NAM remained unsolved, though the presence of susceptibility to malignant hyperthermia as a clinical feature suggested a defect in a component of the EC coupling apparatus. To see if a mutation in *STAC3* was the basis for NAM, *STAC3* coding regions were sequenced in a cohort of 5 NAM families that included 5 affected and 13 unaffected individuals. As expected for an autosomal recessive disorder, all affected individuals were homozygous for a G>C missense mutation of base pair 1046 in exon 10 of the *STAC3* gene (Ensembl transcript ID ENST00000332782), while all obligate carriers were heterozygous. This mutation resulted in a tryptophan (W) to serine (S) substitution at amino acid 284 in the first SH3 domain (Fig. 7). The sequence change perfectly segregated with the NAM phenotype, and was not found in an additional three unaffected, unrelated Lumbee individuals (Supplementary Fig. S8), nor in 113 Caucasian control individuals. In addition, *STAC3* has been sequenced as part of the 1000 genome project, and this mutation has not been detected. This pattern of inheritance suggested that *STAC3* was the basis for the congenital myopathy.

Next the functional consequences of the W284S mutation was investigated in the zebrafish model system. The analogous W>S substitution was encoded in zebrafish *stac3* (*hsp70:stac3*^{NAM}*-egfp*) and expressed in *stac3*^{mi34} null mutant muscles to assay for phenotypic rescue. Unlike *stac3*^{wt}*-egfp*, expression of *stac3*^{NAM}*-egfp* failed to rescue touch induced swimming although some Stac3^{NAM} localized to triads (Fig. 8a). Furthermore, Ca^{2+} imaging of mutant fast but not slow twitch muscles expressing *stac3*^{NAM}*-mCherry* and *GCaMP3* exhibited Ca^{2+} transients that were decreased compared with mutant muscles expressing *stac3*^{wt}*-mCherry* and *GCaMP3* (Fig. 4b, Fig. 8b,c). Presumably the mosaic expression of a partially effective allele was insufficient to result in behavioral rescue.

Decreased Ca^{2+} transients in fast twitch but not slow twitch muscles expressing *stac3*^{NAM} predicts defective swimming since by 48 hpf swimming is dependent on fast twitch muscle contractions and independent of slow twitch contractions[35]. Additionally, expression of wildtype human *STAC3* in mutant zebrafish muscles rescued the motor phenotype (Supplementary Fig. S9). Thus the NAM mutation appeared to diminish EC coupling in fast twitch muscles and was causative for the congenital myopathy.

DISCUSSION

This study identified Stac3 as a novel component of EC coupling in skeletal muscles, and a mutation in STAC3 as the cause for Native American myopathy. A recent study suggested that MO mediated knockdown of *stac3* in zebrafish embryos resulted in defective myofibrillar formation in skeletal muscles[36], but we found that myofibrils in embryonic and larval zebrafish were comparable between *wt* sibs and *stac3* mutants. This discrepancy might be due to the maternal wt *stac3* transcript found in *stac3* nulls, which could have been sufficient for normal myofibrillar formation in mutants.

In principle Stac3 could participate in EC coupling via a variety of mechanisms. One possibility is that Stac3 might modulate the channel properties of DHPR and/or RyR1. The triadic localization of Stac3 and biochemical demonstration that Stac3 is part of the DHPR/RyR1 complex are consistent with this possibility. Regulation of DHPR or RyR1 channel properties by other triadic components include modulation of the properties of DHPR by RyR1 and of RyR1 by FKBP12. In murine RyR1-deficient myotubes the complement of DHPR on the muscle membrane is normal, but the DHPRs pass much less

Ca^{2+} than normal[37]. The immunophilin, FKBP12, copurifies with RyR and anti-FKBP12 can pull down RyR in striated muscles[14]. When RyR were examined with single channel recordings, FKBP12 was found to optimize channel function[15]. The β subunits of voltage-dependent Ca channels are also known to regulate properties of a variety of Ca channels[38]. It is possible that Stac3 could interact with the β_{1a} subunit to regulate DHPR channel properties in skeletal muscles.

Another possibility is that Stac3 may regulate the precise organization of DHPRs and RyR1s at triadic junctions of the t-tubules and SR. At triads DHPRs and RyR1s are organized in a precise manner with DHPRs arranged in geometrically arranged groups of four called tetrads with each tetrad apposed to every other RyR1 homotetramer[39]. The β_{1a} subunit of DHPR also appears to be critical for this since β_{1a} is required for formation of DHPRs into tetrads[23].

Stac3 might also regulate the amount of DHPR and/or RyR1 at triads perhaps by modulating protein trafficking and/or stability of DHPR and/or RyR1. An example of a factor that may be important for trafficking or stability of DHPRs is REM, a member of the RGK GTP-binding protein family. REM can bind β subunits of voltage-dependent Ca^{2+} channels when expressed heterologously and overexpression of REM inhibits L-type Ca^{2+} channels in C2C12 cells[40] and in skeletal muscles due to a decrease of DHPR in the muscle membrane[41] via dynamin dependent endocytosis[42]. Although the loss-of-function phenotype for REM is

not known, these results suggest that REM inhibits localization of DHPRs in triads either by decreasing processing of the channels into triadic junctions or by increasing the removal of the channel from triads. Interestingly the $DHPR_{\beta 1}$ subunit regulates levels of plasmamembrane $DHPR_{\alpha 1c}$ ($Ca_V1.2$) that is expressed by cardiac muscle cells and neurons by inhibiting the degradation of these channels via endoplasmic reticulum-associated protein degradation[43]. Examination of the amount of DHPR and RyR1 at triads in *stac3* mutants versus wildtype muscles should clarify whether Stac3 controls the levels of these key components in skeletal muscles. Furthermore, it should be possible to investigate whether Stac3 regulates protein trafficking of key components of EC coupling using various transgenics combined with live-imaging strategies in zebrafish to directly examine fluorescently labeled EC components as they are trafficked from the ER to triads and as they are endocytotically removed from the triads. Furthermore, the availability of mutants deficient for DHPR [23,29] and RyR1[30] in addition to the *stac3*^{mi34} mutant should be invaluable for mechanistic analysis of Stac3 for EC coupling.

The NAM mutation converted W284 to S in the 1st SH3 domain of Stac3. Interestingly an analysis of binding specificities of SH3 domains using a generic structure based model found that this W, which is in the loop region of the SH3 domain and is highly conserved across SH3 domains, is one of the most important residues for binding specificity[44]. Our finding that expression of $Stac3^{NAM}$ in Stac3 null zebrafish leads to decreased EC coupling suggests that interactions of the 1st SH3 domain in Stac3 is important for normal EC coupling. In fact, components of the triadic molecular complex including $DHPR_{\alpha 1s}$, $DHPR_{\beta 1a}$ and RyR1 contain numerous SH3 binding sequences in their predicted cytoplasmic portions. Thus it would be interesting to see if Stac3 might interact with triadic components such as DHPR and/or RyR1 via the Stac3 SH3 domain and whether such an interaction is necessary for normal EC coupling. Interestingly, the structure based model also identified 3 other residues found in human Stac3 (Y255, E283 and N299) that also significantly affected binding specificity[44]. The roles of these residues for EC coupling could be examined by expressing appropriately mutagenized Stac3 in the zebrafish *stac3* nulls.

Genetic and physiological approaches should also be useful for the generation of transgenic lines of *stac3*^{NAM} mutant zebrafish to delineate the pathology of NAM and for identifying potential therapeutic agents. This is particularly relevant given the increasing recognition of mutations in genes associated with EC coupling in a growing range of human muscle diseases. In addition, *STAC3* is an attractive candidate for the genetic basis of currently undefined congenital myopathies, particularly those associated with susceptibility to malignant hyperthermia and/or those with phenotypes similar to those of patients with *RYR1* or *DHPR* mutations.

METHODS

Animals and Behavioral Analysis

Zebrafish were bred and maintained according to approved guidelines of the University Committee on Use and Care of Animals at the University of Michigan. The *stac3*^{mi34} mutation was isolated from a mutagenesis screen using procedures previously reported[19, 20].

Embryonic behaviors were video-recorded mounted on a stereomicroscope and analyzed with ImageJ. In some cases the heads of embryos were embedded in low melting temp agar with the trunk and tail free to move. Where indicated data were analyzed by t-tests.

Electrophysiology

Previously published protocols were followed to electrophysiologically record from zebrafish embryonic muscles[21]. For recordings embryos were partially curarized (6 μM d-tubocurarine). Recordings of muscle responses to touch were made with patch electrodes (3–10 MΩ) filled with solution containing 105 mM K gluconate, 16 mM KCl, 2 mM $MgCl_2$, 10 mM Hepes, 10 mM EGTA and 4 mM Na_3ATP at 273 mOsm and pH 7.2 and extracellular Evans solution (134 mM NaCl, 2.9 mM KCl, 2.1 mM $CaCl_2$, 1.2 mM $MgCl_2$, 10 mM glucose and 10 mM Hepes at 290 mOsm and pH 7.8) using an Axopatch 200B amplifier (Axon Instruments), low-pass filtered at 5 kHz and sampled at 1 kHz. Mechanosensory stimulation was delivered by ejecting bath solution from a pipette using a Picospritzer. Voltage dependence of contraction was performed in a similar fashion except embryos were exposed to 50 μM d-tubocurarine, voltage steps delivered to muscle via voltage clamp and muscle contractions video-recorded at 60Hz. Muscle contractions to caffeine applied by a Picospritzer (10 psi, 1 sec) of dissected embryos were video-recorded and measured.

Ca^{2+} Imaging

One cell stage embryos were injected with a plasmid using α-actin promoter[29] (*α-actin:GCaMP3*) resulting in.embryos that mosaically expressed *α-actin:GCaMP3* within skeletal muscle. 48 hpf embryos were genotyped by behavior. Prior to imaging tricaine was removed and embryos allowed to recover in Evans for 10 minutes and treated with 200 μM N-benzyl-p-toluene sulphonamide to inhibit contraction for 5 minutes. 100 μM NMDA was added to initiate the swimming motor network[17]. GCaMP3 expressing cells were frame scanned at 200Hz using the resonance scanner of a Leica SP5 confocal microscope. Confocal software was used to measure relative fluorescence intensity changes and kinetics of induced Ca^{2+} transients.

Immunolabeling

Wholemounted embryos were immunolabeled as described previously[26]. For labeling dissociated skeletal muscle fibers, 48 hpf embryos were incubated in collagenase type II (3.125 mg/ml in CO_2-independent medium) at 20°C for 1.5 h with the muscle fibers triturated every 30 min. Fibers were spun at 380*g* for 5 min, supernatant removed and fibers resuspended and allowed to settle on polyornithine coated coverslips. Fibers were washed then fixed. Dissociated muscles were labeled using 0.25% detergent in the incubation solutions containing the following primary antibodies/toxin: 1/200 dilution of anti-RyR (34C IgG1, Sigma); 1/200 anti-$DHPR_{\alpha 1}$ (1A IgG1, Affinity BioReagents);1/10 bungarotoxin-Alexa594 (Invitrogen); 1/500 anti-SV2; 1/200 anti-α actinin; and 1/200 anti-dystrophin (all from Iowa Hybridoma Bank). In some cases nuclei were labeled with 0.1% DAPI.

Positional Cloning of *stac3*

To identify the gene mutated in *stac3*^{mi34} mutants, the mutation was meiotically mapped to PCR-scorable, polymorphic CA repeats as described previously[45] by scoring 2009 mutant embryos derived from appropriate mapping crosses. Flanking markers were identified located on linkage group 9; z1830 that was 0.21 cM north of *stac3*^{mi34} and z1663 that was 1.24 cM south. Analysis of the zebrafish genome database (http://www.sanger.ac.uk/Projects/Drerio/clones.shtml) revealed that z1830 was located in a small contig of assembled sequence (Scaffold 450) from the zV5 assembly of the sequenced genome that contained the *pcbp2* gene. A new marker (zh1) located in *pcbp2* mapped 0.11 cM north of *stac3*^{mi34}. A sequenced 156 kb BAC (CR848672) that contained *pcbp2* was identified and analyzed for potential genes with the gene prediction program, GENSCAN (http://genes.mit.edu/GENSCAN.html), and BLASTing predicted genes against the NCBI database (http://www.ncbi.nlm.nih.gov/BLAST). These were *pcbp2*, *kif5a*, *arp5* and a gene similar to *stac*. New markers, zh34 in *kif5a* (0.04 cM north), zh16 in *arp5* (0.04 cM south) and zh31 in the *stac*-like gene (no recombinants), were identified. The *stac*-like cDNA from wildtype and mutant embryos were isolated and sequenced and the mutant cDNA contained an insertion that included an in frame stop codon. Analysis of genomic sequences determined that the *stac3*^{mi34} allele contained a missense mutation that transformed a splice donor site for the intron between exon 4 and exon 5 (GT to AT) that presumably lead to incorrect splicing and inclusion of the intron in the cDNA.

Mutant Rescue

Rescue of *stac3*^{mi34} behavior was performed by subcloning zebrafish *stac3*^{wt}, *stac3*^{mi34}, *stac3*^{NAM} or human *STAC3* into *pHSP70-EGFP*[42]. Zebrafish *stac3*^{NAM} construct was generated by site-directed mutagenesis. Constructs (10 ng/μl) were injected into one cell stage progeny of *stac3*^{mi34} carriers with a Nanoject II. At 48 hpf *stac3*^{mi34} mutant embryos were behaviorally identified and heat induced by switching them from water at 28.5°C to 37°C for 1 h. Following heat induction embryos were switched back to 28.5°C and assayed 3 and 24 h later. Embryos with approximately 10% or more skeletal muscle fibers expressing EGFP were used for behavioral assays. Responses of embryos to touch were video-recorded and measured. For Ca^{2+} imaging of Stac3^{wt} or Stac^{NAM} expressing muscle fibers *pHSP70:stac3*^{wt}*-mCherry* and *pHSP70:stac3*^{NAM}*-mCherry* were generated along with *α-actin:GCaMP3*. Embryos were injected with a 1:1 mixture of a *stac3* construct and *α-actin:GCaMP3* each at 10ng/μl. Following heat induction embryos with skeletal muscle fibers expressing both constructs were selected for Ca^{2+} imaging.

Analysis of Maternal Transcripts by RT-PCR

The start of mid-blastula transition and earlieat zygotic transcription is at 3 hpf in zebrafish[34]. 50 embryos at 2 and 3 hpf each were placed in Trizol and RT-PCR was performed for *stac3* and *tuba1* (*tubulin α1*), a housekeeping gene that is maternally expressed[46]. Exon-overlapping primer pairs shown below were designed to amplify ~200bp fragments of cDNA from the 5′ (representing exons 3–6) or 3′ (exons 4–10) region of mature *stac3* message.

5′ primer pair

forward: 5′-GGACGACAACACTGTGTATTTTGTGTATG-3′

reverse: 5′-GAACCCAGGAGGTATTTTGCCGAAGCATCT-3′

3′ primer pair

forward: 5′-ACGGATGATTGTTCTCAATAATAAGTTTGC-3′

reverse: 5′-CGCAACAGATGACAAGAACAAGAAGCAG-3′

Antisense Morpholino Oligonucleotide Knockdowns

4.6 nL of 400 μM solutions of translation blocking antisense MO (GeneTools) or standard control MO were injected into recently fertilized embryos from crosses of *stac3*^{mi34} carriers using a Nanoject II. The sequence of the antisense stac3 MO was: 5′-TCATATTGAGC**CAT**CAGTCCAGC-3′ with **CAT** corresponding the start ATG. For morphant rescue experiments 10 ng/μL of *α-actin:stac3-egfp* was coinjected along with the antisense MOs. Embryos were assayed for response to touch with forceps at 48hpf and subsequently fixed and assayed with anti-Stac3.

Polyclonal Antiserum Production and Purification

Full-length zebrafish Stac3 was expressed as a His-Sumo fusion protein in B21(DE3) cells (Invitrogen), and affinity-purified using Ni-NTA agarose. Protein was further purified by electrophoresis in a NuPAGE 4–12% SDS-PAGE Bis-Tris Gel and subsequent excision of appropriate Coomassie stained band. Rabbits were immunized with gel slices of purified fusion proteins. Antiserum was purified by passing through a Sulfolink column (Thermo) containing the immobilized fusion protein. Fragment of Stac3 that was bound by anti-Stac3 was identified as follows. Full-length *stac3* cDNA and the fragment that encodes amino acids 1–63 were cloned in frame into pGADGT7 (Clontech) which contains an N-terminal HA tag and Gal4 activation domain. Each construct was transformed into Y2HGold Yeast using Yeastmaker Yeast Transformation system 2 (Clontech) and plated on appropriate auxotrophic media. Yeast was grown, harvested, and protein extracted with YPER yeast protein extraction reagent (Thermo). Protein samples were loaded for SDS-PAGE analysis, blotted onto nitrocellulose, and probed separately with anti-HA or anti-Stac3.

Western Analysis and Immunoprecipitation

50 *stac3*^{mi34} mutant and sibling embryos each were collected, lysed and the isolated protein loaded and separated by SDS/PAGE[22]. Anti-DHPR$_{\alpha 1}$ was used for immunoblotting at 1:500, anti-pan-RyR at 1:2000. Adult female fish were sacrificed using 0.1% tricaine, skeletal muscle dissected on dry ice, and total protein extracted. Protein lysate from an individual fish was immunoprecipitated using anti-DHPR$_{\alpha 1}$ (1:100), or anti-pan-RyR (1:200) crosslinked with BS^3 (Thermo) to Protein G Dynabeads (Invitrogen).

Generation of Stable Transgenic Line

α-*actin:stac3-gfp* construct was injected at 20 ng/μl into the cytoplasm of embryos at the 1-cell stage. Fish were raised to adulthood and germline founders identified by screening F1 progeny for GFP fluorescence. GFP-positive offspring were raised to establish the transgenic line.

Mass Spectrometry and Data Analysis

Skeletal muscle lysates from 10 adult α-*actin:stac3-gfp* transgenic fish were pooled for immunoprecipitation with anti-GFP (Torrey Pines Biolabs Inc.) or Normal Mouse IgG. The pulldown fraction was separated using SDS-PAGE, and the fractions in the gel stained using Silver Stain Kit (Pierce). Thirteen bands appearing in the anti-GFP pulldown fraction lane but not in normal IgG pulldown lane were excised, washed with 25 mM ammonium bicarbonate followed by acetonitrile, reduced with 10 mM dithiothreitol at 60°C followed by alkylation with 50 mM iodoacetamide at RT, and digested with trypsin at 37°C for 4 hours. Mass spectrometry was performed by the University of Michigan Proteomics and Peptide Synthesis Core using a nano LC/MS/MS with a Waters NanoAcquity HPLC system interfaced to a ThermoFisher LTQ Orbitrap Velos. Peptides were loaded on a trapping column and eluted over a 75 μm analytical column at 350 nL/min; both columns were packed with Jupiter Proteo resin (Phenomenex). The mass spectrometer was operated in data-dependent mode, with MS performed in the Orbitrap at 60,000 FWHM resolution and MS/MS performed in the LTQ. The fifteen most abundant ions were selected for MS/MS.

MS/MS samples were analyzed using Mascot (Matrix Science, London). Mascot was set up to search the ipi.DANRE.v3.75.decoy database (74790 entries). Mascot was searched with a fragment ion mass tolerance of 0.50 Da and a parent ion tolerance of 10.0 PPM. Carbamidomethyl of cysteine was specified in Mascot as a fixed modification.

Scaffold (version Scaffold_3.1.2, Proteome Software Inc., Portland, OR) was used to validate MS/MS based peptide and protein identifications. Peptides were identified at greater than 95% probability and proteins were identified if they contained at least two identified peptides with each peptide identified in the protein at greater than 95% probability. Peptide and protein probabilities were assigned by the Protein Prophet algorithm[47]. Proteins that contained similar peptides and could not be differentiated based on MS/MS analysis alone were grouped to satisfy the principles of parsimony.

Molecular Analysis of Native American Myopathy

The cohort of individuals with NAM was previously described[34]. NAM subjects were of Lumbee Indian descent with congenital muscle weakness who demonstrate two of more of the following phenotypic characteristics: myopathic facies, susceptibility to malignant hyperthermia, kyphoscoliosis, and cleft palate. The probands were ascertained from the University of North Carolina at Chapel Hill Pediatric Genetics Clinic and from the Duke University Muscular Dystrophy Clinic. All data and samples were collected following informed consent of subjects; this study was approved by the Duke University Medical Center and the University of North Carolina Institutional Review Boards. DNA was extracted from whole blood using the Puregene system (Gentra Systems, Minneapolis, MN) and stored in the laboratory of the Duke Center for Human Genetics.

Initially, each exon and the surrounding splicing regions of *STAC3* were screened in 3 NAM patients and 3 related individuals through PCR amplification and automated Sanger sequencing. After identification of the NAM mutation in exon 10 of *STAC3*, the entire cohort of available samples from NAM pedigrees was screened by exon amplification and

sequencing for the mutation. In all, a total of 18 individuals from 5 Lumbee families were sequenced, as well as 3 unrelated unaffected Lumbee individuals. In addition, genomic DNA was screened from 2 neurologically normal control individuals (Coriell Institute NDPT006 and NDPT009) and from a collection of 111 adult subjects without evidence of neurological disease[48].

Electron Microscopy

Transmission electron microscopy was performed as previously described[7,49]. A minimum of 3 larvae per condition were examined.

Supplementary Material

Refer to Web version on PubMed Central for supplementary material.

Acknowledgments

The authors thank Dr. H. Xu (University of Michigan) for discussions of the experiments, B. Wagner, E. Andraska, M. Lacey and A. Migda for collecting and raising *stac3*^{mi34} embryos, T. Waugh and T. Tubbs for assistance with human *STAC3* screening, Drs. H. Okamoto (RIKEN, Japan) and L. Looger (Janelia Farms, HHMI) for plasmid constructs, Dr. Hienriette Remmer (University of Michigan) for advise on mass spectrometry and data analysis and the patients and families who provided biological samples. Research was supported by grants from NINDS (RO1NS54731) and NSF (0725976) to J.Y.K., NIAMS (1K08AR054835) and the Taubman Medical Institute to J.J.D., the Muscular Dystrophy Association (MDA186447) to M.A.H. and NIAMS (RO1HL048093) to C.F.-A. H.H. was supported by a Long-Term Fellowship and a Career Development Award from the Human Frontier Science Program, W.W.C. in part by a Center for Organogenesis Training Grant (NIH T32-HD007505), J.W.L. by the Cell and Molecular Biology Training Grant (NIH T32-GM-07315) and a Rackham Merit Fellowship from the University of Michigan.

References

1. Sewry CA, Jimenez-Mallebrera C, Muntoni F. Congenital myopathies. Curr Opin Neurol. 2008; 5:569–575. [PubMed: 18769251]
2. Rios E, Brum G. Involvement of dihydropyridine receptors in excitation-contraction coupling in skeletal muscle. Nature. 1987; 325:717–720. [PubMed: 2434854]
3. Tanabe T, Takeshima H, Mikami A, Flockerzi V, Takahashi H, Kangawa K, Kojima M, Mastuo H, Hirose T, Numa S. Primary structure of the receptor for calcium channel blockers from skeletal muscle. Nature. 1987; 328:313–318. [PubMed: 3037387]
4. Adams BA, Tanabe T, Mikami A, Numa S, Beam KG. Intramembrane charge movement restored in dysgenic skeletal muscle by injection of dihydropyridine receptor cDNAs. Nature. 346:569–572. [PubMed: 2165571]
5. Bannister RA. Bridging the myoplasmic gap: recent developments in skeletal muscle excitation-contraction coupling. J Muscle Res Cell Motil. 2007; 28:275–283. [PubMed: 17899404]
6. Takeshima H, Nishimura S, Matsumoto T, Ishida H, Kangawa K, Minamino N, Matsuo H, Ueda M, Hanaoka M, Hirose T, Numa S. Primary structure and expression from complementary DNA of skeletal muscle ryanodine receptor. Nature. 1989; 339:439–445. [PubMed: 2725677]
7. Block BA, Imagawa T, Campbell KP, Franzini-Armstrong C. Structural evidence for direct interactions between the molecular components of the transverse tubule/sarcoplasmic reticulum junction in skeletal muscle. J Cell Biol. 1988; 107:2587–2600. [PubMed: 2849609]
8. Paolini C, Fessenden JD, Pessah IN, Franzini-Armstrong C. Evidence for conformational coupling between two calcium channels. Proc Natl Acad Sci. 1994; 101:12748–12752. [PubMed: 15310845]
9. Lanner JT, Georgiou DK, Joshi AD, Hamilton SL. Ryanodine receptors: structure, expression, molecular details, and function in Ca release. Cold Spring Harb Perspect Biol. 2010; 2:a003996. [PubMed: 20961976]

10. Gonzales-Serratos R, Valee-Aguilera R, Lathrop DA, del Carmen Garcia M. Slow inward calcium currents have no obvious role in muscle excitation-contraction coupling. Nature. 1982; 298:292–294. [PubMed: 6806669]
11. Schredelseker J, Shrivastav M, Dayal A, Grabner M. Non-Ca^{2+}-conducting channels in fish skeletal muscle excitation-contraction coupling. Proc Natl Acad Sci. 2010; 107:5658–56663. [PubMed: 20212109]
12. Beard NA, Laver DR, Dulhunty AF. Calsequestrin and the calcium release channel of skeletal and cardiac muscle. Prog Biophys Mol Biol. 2004; 85:33–69. [PubMed: 15050380]
13. Knollmann BC, Chopra N, Hlaing T, Akin G, Yang T, Ettensohn K, Knollman BE, Horton KD, Weissman NJ, Holinstat I, Zhang W, Roden DM, Jones LR, Franzini-Armstrong C, Pfeifer K. Casq2 deletion causes sarcoplasmic reticulum volume increase, premature Ca^{2+} release, and catecholaminergic polymorphic ventricular tachycardia. J Clin Invest. 2006; 116:2510–2520. [PubMed: 16932808]
14. Chopra N, Yang T, Asghari P, Moore ED, Huke S, Akin B, Cattolica RA, Perez CF, Hlaing T, Knollmann-Ritschel BE, Jones LR, Pessah IN, Allen PD, Franzini-Armstrong C, Knollmann BC. Ablation of triadin causes loss of Ca^{2+} release units, impaired excitation-contraction coupling, and cardiac arrhythmias. Proc Natl Acad Sci USA. 2009; 106:7636–7641. [PubMed: 19383796]
15. Jayaraman T, Brillantes AM, Timerman AP, Fleischer S, Erdjument-Bromage H, Tempst P, Marks AR. FK506 binding protein associated with the calcium release channel (ryanodine receptor). J Biol Chem. 1992; 268:9474–9477. [PubMed: 1374404]
16. Brillantes AB, Ondrias K, Scott A, Kobrinsky E, Ondriasova Em, Moschella MC, Jayaraman T, Landers M, Erhlich BE, Marks AR. Stabilization of calcium release channel (ryanodine receptor) function by FK506-binding protein. Cell. 1994; 77:513–523. [PubMed: 7514503]
17. Moghadaszadeh B, Petit Nm, Jaillard C, Brockington M, Quijano Roy S, Merlini L, Romero N, Estournet B, Desguerre I, Chaigne D, Muntoni F, Topaloglu H, Guicheney P. Mutations in SEPN1 cause congenital muscular dystrophy with spinal rigidity and restrictive respiratory syndrome. Nat Genet. 2001; 29:17–18. [PubMed: 11528383]
18. Jurynec MJ, Xia R, Macrill JJ, Gunther D, Crawford T, Flanigan KM, Abramson JJ, Howard MT, Grunwald DJ. Selenoprotein N is required for ryanodine receptor calcium release channel activity in human and zebrafish muscle. Proc Natl Acad Sci USA. 2008; 105:12485–12490. [PubMed: 18713863]
19. Halling DB, Aracena-Parks P, Hamilton SL. Regulation of voltage-gated Ca^{2+} channels by calmodulin. Science STKE. Jan 17.2006
20. Haffter P, Granato M, Brand M, Mullins MC, Hammerschmidt M, Kane DA, Odenthal J, van Eeden FJ, Jiang YJ, Heisenberg CP, Kelsh RN, Furutani-Seiki M, Vogelsang E, Beuchle D, Schach U, Fabian C, Nüsslein-Volhard C. The identification of genes with unique and essential functions in the development of the zebrafish, *Danio rerio*. Development. 1996; 123:1–36. [PubMed: 9007226]
21. Driever W, Solnica-Krezel L, Schier AF, Neuhauss SC, Malicki J, Stemple DL, Stainier DY, Zwartkruis F, Abdelilah S, Rangini Z, Belak J, Boggs C. A genetic screen for mutations affecting embryogenesis in zebrafish. Development. 1996; 123:37–46. [PubMed: 9007227]
22. Buss RR, Drapeau P. Physiological properties of zebrafish embryonic red and white muscle fibers during early development. J Neurophysiol. 2000; 84:1545–1557. [PubMed: 10980026]
23. Schredelseker J, Di Biase V, Obermair GJ, Felder ET, Flucher BE, Franzini-Armstrong C, Grabner M. The β_{1a} subunit is essential for the assembly of dihydropyridine receptor arrays in skeletal muscle. Proc Natl Acad Sci USA. 2005; 102:17219–17224. [PubMed: 16286639]
24. Stamm DS, Aylsworth AS, Stajich JM, Kahler SG, Thorne LB, Speer MC, Powell CM. Native American Myopathy: congenital myopathy with cleft palate, skeletal anomalies, and susceptibility to malignant hyperthermia. Am J Med Genet A. 2008; 146A:1832–1841. [PubMed: 18553514]
25. Stamm DS, Powell CM, Stajich JM, Zismann VL, Stephan DA, Chesnut B, Aylsworth AS, Kahler SG, Deak KL, Gilbert JR, Speer MC. Novel congenital myopathy locus identified in Native American Indians at 12q13.13–14.1. Neurology. 2008; 71:1764–1769. [PubMed: 18843099]

26. Hirata H, Saint-Amant L, Waterbury J, Cui W, Zhou W, Li Q, Goldman DJ, Granato M, Kuwada JY. *accordion*, a zebrafish behavioral mutant, has a muscle relaxation defect due to a mutation in the ATPase calcium pump SERCA1. Development. 2004; 131:5457–5468. [PubMed: 15469975]
27. Hirata H, Saint-Amant L, Downes GB, Cui WW, Zhou W, Granato M, Kuwada JY. Zebrafish *bandoneon* mutants display behavioral defects due to a mutation in the glycine receptor b subunit. Proc Natl Acad Sci USA. 2005; 102:8345–8350. [PubMed: 15928085]
28. Cui WW, Low S, Hirata H, Geisler R, Hume RI, Kuwada JY. The zebrafish *sho* gene encodes a glycine transporter and is essential for the function of early neural circuits in the CNS. J Neurosci. 2005; 25:6610–6620. [PubMed: 16014722]
29. Zhou W, Shirabe K, Thisse C, Thisse B, Kuwada JY. Non-sense mutations in the dihydropyridine receptor β1 gene, *CACNB1*, paralyze zebrafish *relaxed* mutants. Cell Calcium. 2006; 39:227–236. [PubMed: 16368137]
30. Hirata H, Watanabe T, Hatakeyama J, Sprague SM, Saint-Amant L, Nagashima A, Cui WW, Zhou W, Kuwada JY. Zebrafish*relatively-relaxed* mutants have a ryanodine receptor defect, exhibit slow swimming and provide a model of multi-minicore disease. Development. 2007; 134:2771–2781. [PubMed: 17596281]
31. Saint-Amant L, Drapeau P. Time course of the development of motor behaviors in the zebrafish embryo. J Neurobiol. 1998; 37:622–632. [PubMed: 9858263]
32. Tian L, Hires SA, Mao T, Huber D, Chiappe ME, Chalasani SH, Petreanu L, Akerboom J, McKinney SA, Schreiter ER, Bargmann CI, Jayaraman V, Svoboda K, Looger LL. Imaging neural activity in worms, flies and mice with improved GCaMP calcium indicators. Nat Methods. 2009; 6:875–881. [PubMed: 19898485]
33. Suzuki H, Kawai J, Taga C, Yaoi T, Hara A, Hirose K, Hayashizaki Y, Watanabe S. Stac, a novel neuron-specific protein with cysteine-rich and SH3 domains. Biochem Biophys Res Commun. 1996; 229:902–909. [PubMed: 8954993]
34. Kane DA, Kimmel CB. The zebrafish midblastula transition. Development. 1993; 119:447–456. [PubMed: 8287796]
35. Nanagawa Y, Hirata H. Developmental transition of touch response from slow muscle-mediated coiling to fast muscle-mediated burst swimming in zebrafish. Dev Biol. 2011; 355:194–204. [PubMed: 21554867]
36. Bower NI, Garcia de la serrana D, Cole NJ, Hollway GE, Lee H-T, Assinder S, Johnston IA. Stac3 is required for myotube formation and myogenic differentiation in vertebrate skeletal muscle. J Biol Chem. 2012; 287:43936–43949. [PubMed: 23076145]
37. Nakai J, Dirksen RT, Nguyen HT, Pessah IN, Beam KG, Allen PD. Enhanced dihydropyridine receptor channel activity in the presence of ryanodine receptor. Nature. 1996; 380:72–75. [PubMed: 8598910]
38. Dolphin AC. β subunits of voltage-gated calcium channels. J Bioenerg Biomem. 2003; 35:599–620.
39. Block BA, Imagawa T, Campbell KP, Franzini-Armstrong C. Structural evidence for direct interaction between the molecular components of the transverse tubule/sarcoplasmic reticulum junction in skeletal muscle. J Cell Biol. 1988; 107:2587–2600. [PubMed: 2849609]
40. Finlin BS, Crump SM, Satin J, Andres DA. Regulation of voltage-gated calcium channel activity by the REM and Rad GTPases. Proc Natl Acad Sci. 2003; 100:14469–14474. [PubMed: 14623965]
41. Bannister RA, Colecraft HM, Beam KG. Rem inhibits skeletal muscle EC coupling by reducing the number of functional L-type Ca^{2+} channels. Biophys J. 2008; 94:2631–2638. [PubMed: 18192376]
42. Yang T, Xu X, Kernan T, Wu V, Colecraft HM. Rem, a member of the RGK GTPases, inhibits recombinant $Ca_V1.2$ channels using multiple mechanisms that require distinct conformations of the GTPases. J Physiol. 2010; 588:1665–1681. [PubMed: 20308247]
43. Altier C, Garcia-Caballero A, Simms B, You H, Chen L, Walcher J, Tedford HW, Hermosilla T, Zamponi GW. The Cavβ subunit prevents RFP2-mediated ubiquitination and proteosomal degradation of L-type channels. Nat Neurosci. 2011; 14:173–180. [PubMed: 21186355]

44. Hou T, Xu Z, Zhang W, McLaughlin WA, Case DA, Xu Y, Wang W. Characterization of domain-peptide interaction interface. Mol Cell Proteomics. 2009; 8.4:639–649. [PubMed: 19023120]

45. Shimoda N, Knapik EW, Ziniti J, Sim C, Yamada E, Kaplan S, Jackson D, de Sauvage F, Jacob H, Fishman MC. Zebrafish genetic map with 2000 microsatellite markers. Genomics. 1999; 58:219–232. [PubMed: 10373319]

46. Callard GV, McCurley AT. Characterization of housekeeping genes in zebrafish: male-female differences and effects of tissue type, developmental stage and chemical treatment. BMC Mol Biol. 2008; 9:102. [PubMed: 19014500]

47. Nesvizhskii AI, Keller A, Kolker E, Aebersold R. A statistical model for identifying proteins by tandem mass spectrometry. Anal Chem. 2003; 75:4646–58. [PubMed: 14632076]

48. Rainier S, Sher C, Reish O, Thomas D, Fink JK. *De novo* occurrence of novel *SPG3A*/atlastin mutation presenting as cerebral palsy. Arch Neurol. 2006; 63:445–447. [PubMed: 16533974]

49. Dowling JJ, Vreede AP, Low SE, Gibbs EM, Kuwada JY, Bonnemann CG, Feldman EL. Loss of myotubularin function results in T-tubule disorganization in zebrafish and human myotubular myopathy. PLoS Genetics. 2009; 5:e1000372. [PubMed: 19197364]

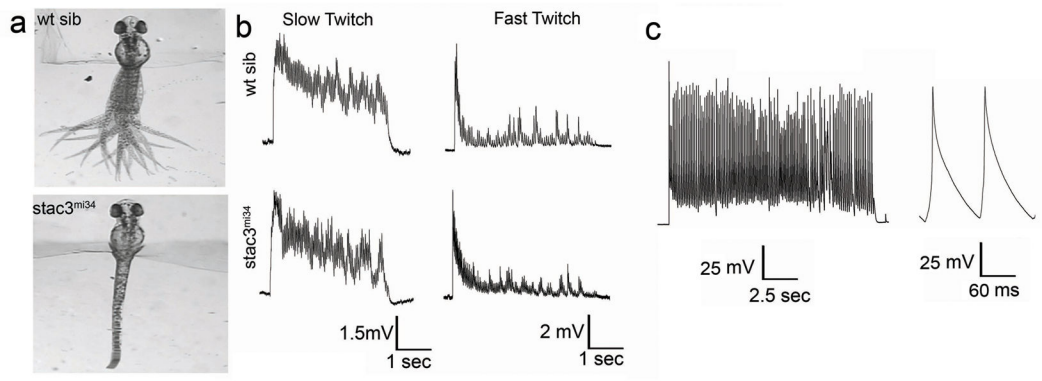

Fig. 1. *mi34* Mutant Zebrafish Exhibit Defective Swimming but CNS Output is Normal

(a) Touch evoked swimming in wt but not *stac3*^{mi34} embryos (48 hpf). Panels show superimposed frames (30 Hz) of swimming motion from wt sibling and *stac3*^{mi34} embryos with heads embedded in agar. (b) Voltage recordings with 6 mM curare showing that touch evoked synaptic responses of slow twitch (wt sib: n=5; mut: n=6) and fast twitch muscles (wt sib: n=6; mut: n=4) of wt sibling and *stac3*^{mi34} mutants (48 hpf) are comparable. Arrowhead denotes tactile stimulation. (c) Voltage recordings with no curare showing that mutant fast twitch muscles (48 hpf) respond to tactile stimulation with a burst of action potentials (n=8).

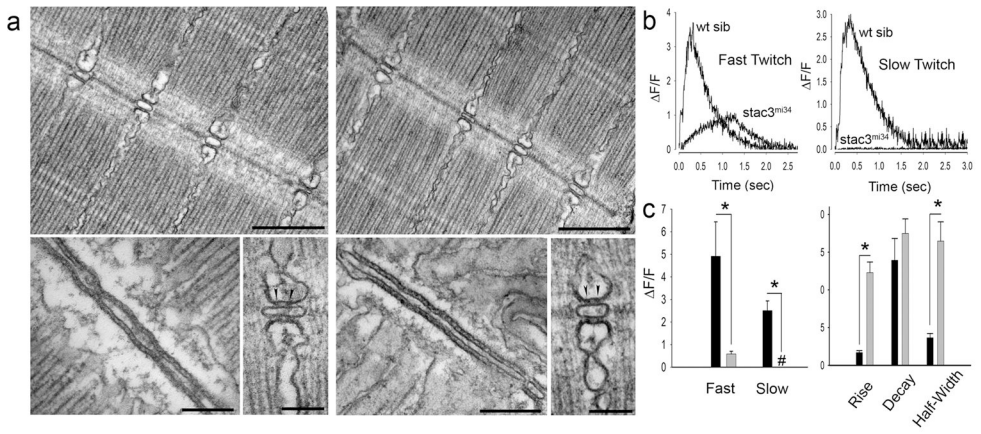

Fig. 2. EC Coupling is Defective in *mi34* Mutant zebrafish Embryos

Electron micrographs showing that the ultrastructure of myofibrils and triadic junctions are comparable between the muscles of 4 dpf wt sibling (a, left) and *mi34* mutants (a, right). Top: Longitudinal sections showing several myofibrils and triads sectioned at right angle to the T tubule long axis. Scale: 500 nm. Bottom: at left a section tangent to the triad, showing one of the two long rows of feet (RyR) that occupy the junctional gap. Scale: 250 nm. Bottom: at right a section transverse to the triad axis showing two feet (arrowheads) in the junctional gap of the triad. Scale: 100 nm. (b) Ca^{2+} transients recorded from GCaMP3 expressing fast and slow twitch fibers are significantly decreased and slower in 48 hpf *stac3*^{mi34} mutants. (c) Left: quantification of peak Ca^{2+} release with black and gray bars representing wt sib (fast, n=5; slow, n=5) and *stac3*^{mi34} (fast, n=9; slow, n=7) fibers, respectively. # denotes that peak Ca^{2+} was 0. Right: quantification of Ca^{2+} transient kinetics in fast fibers with black and gray bars representing wt sib and *stac3*^{mi34}, respectively. Half width denotes the duration the transient is greater than 50% of peak value. Error bars represent standard error of the means. Asterisks signifies $p<0.01$, t-test.

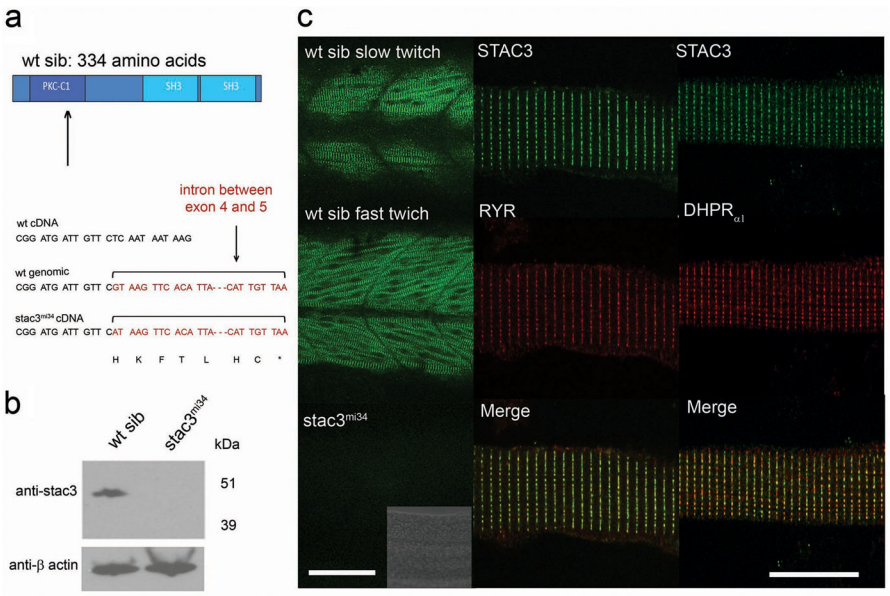

Fig. 3. The Muscle-Specific Gene *stac3* underlies the *mi34* Phenotype

(a) Diagram of the predicted wt Stac3 protein (top). Arrow denotes location of the stop codon. DNA sequence of corresponding regions of wt cDNA, wt genomic DNA, and *stac3*^{mi34} cDNA showing that a missense mutation in a splice donor site lead to the inclusion of the intron (bracket) and stop codon (asterisk) in the mutant cDNA. (b) Stac3 protein appears not to be synthesized in mutants. Western blot of showing that anti-Stac3 labels a band from wt but not mutant embryos at 48 hpf. β actin was the loading control. (c) Stac3 co-localizes with RyR and DHPR$_{\alpha 1}$ in skeletal muscles. Left, side view of the trunk of 48 hpf embryos labeled with anti-Stac3 showing that both fast twitch and slow twitch express Stac3 in wt but not mutant embryos. Scale: 60 μm. Inset shows the brightfield image of the trunk of the mutant. Right, dissociated 48 hpf wildtype muscle fibers labeled with anti-Stac3 and anti-RyR or anti-DHPR$_{\alpha 1}$ showing that Stac3 co-localizes with RyR and DHPRα1. Scale: 10 μm.

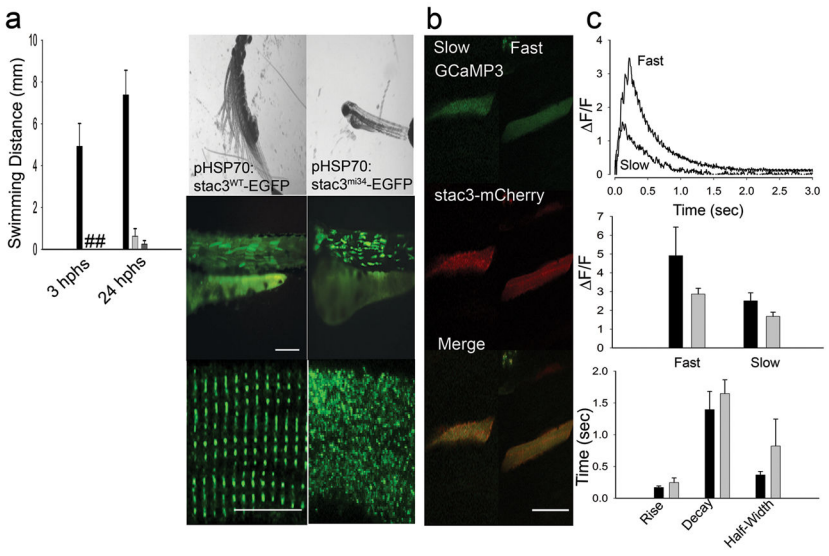

Fig. 4. Expression of wt Stac3 in Muscles Rescues the *stac3*^{mi34} Phenotype

(a) Left, histogram showing that mutant embryos expressing heat inducible *stac3*^{wt}*-egfp* (black, n=32) but not *stac3*^{mi34}*-egfp* (light gray, n=4) nor uninjected mutant embryos (dark gray, n=10) exhibited touch evoked swimming at both 3 h post heat shock (hphs) and 24 hphs. # denotes no swimming. Right panels, superimposed frames (30 Hz, 1 sec) (top) show that mutant embryos expressing *stac3*^{wt} but not *stac3*^{mi34} swim in response to touch although both are similarly expressed by muscles (middle, scale: 180 μm). In dissociated mutant muscles Stac3^{wt}-EGFP localizes to the triads but not Stac3^{mi34}-EGFP (bottom, scale: 10 μm). (b) *In vivo* expression of Stac3^{wt}-mCherry by mutant muscle fibers rescues Ca^{2+} transients. Left panels, *stac3*^{mi34} mutant slow and fast twitch fibers co-expressing *α-actin* driven GCaMP3 and heat induced Stac3^{wt}-mCherry. The triadic localization of Stac3^{wt}-mCherry cannot be seen due to the low resolution of the resonance scans used to detect the fluorescent proteins. (c) Top, Ca^{2+} transients from mutant fast and slow fibers co-expressing Stac3^{wt}-mCherry and GCaMP3. Middle, histogram showing that peak Ca^{2+} release is comparable between wt (black) fast (n=5) and slow (n=5) fibers and rescued mutant (gray) fast (n=6) and slow (n=2) fibers. Bottom, histogram showing that the kinetics of Ca^{2+} transients from wt (black) and rescued mutant (gray) fast twitch fibers are comparable. Error bars represent standard error of the means.

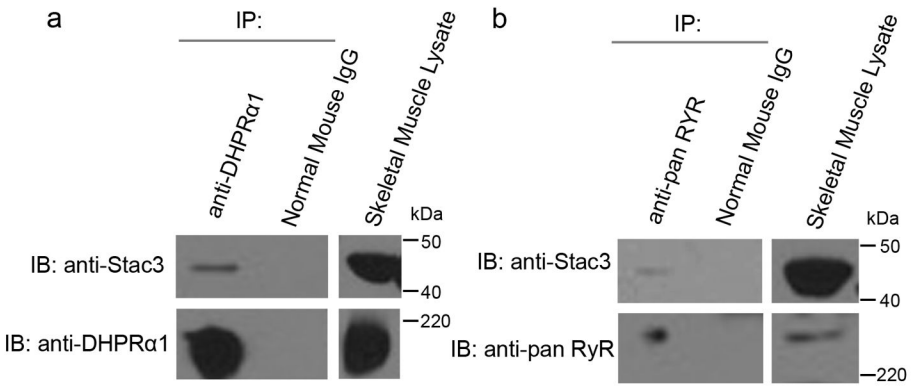

Fig. 5. Stac3 forms a Molecular Complex with DHPR and RyR

(a) Immunoblots (IB) showing that immunoprecipitation (IP) with anti-DHPR$_{\alpha 1}$ but not mouse IgG pulls down DHPR$_{\alpha 1}$ and Stac3 from adult skeletal muscle lysate (n=3). Skeletal muscle lysate lane is a immunoblot showing Stac3 and DHPR$_{\alpha 1}$ are expressed by muscles. (b) Immunoblots showing that immunoprecipitation with anti-pan RyR but not mouse IgG pulls down RyR and Stac3 from adult skeletal muscle lysate (n=3). Skeletal muscle lysate lane is a immunoblot showing Stac3 and RyR are expressed by muscles.

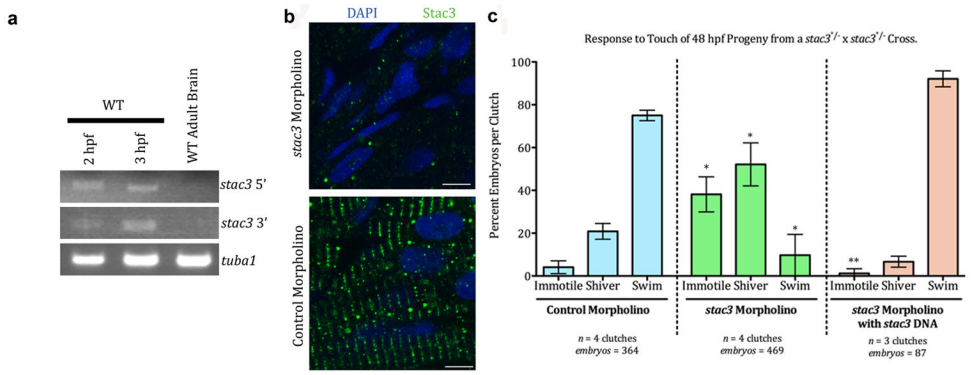

Fig. 6. *stac3* mRNA is Maternally Expressed

(a) RT-PCR from 2 and 3 hpf embryos showing that *stac3* mRNA is maternally expressed. Midblastula transition starts at 3 hpf. *stac3* mRNA is not expressed in adult brain. *tuba1*, a house-keeping gene that is maternally expressed serves as a positive control and *stac3* in adult brain as a negative control. *stac3* 5′ and 3′ refer to primers used for amplifying either 5′ or 3′ fragments of *stac3* from *stac3* cDNA (see Methods). (b) Micrographs showing anti-Stac3 labeled embryos (48 hpf) that had been injected with *stac3* antisense MO (top) but not control MO (bottom) exhibit little to no Stac3. Muscle nuclei are labeled with DAPI (blue). Scale: 5 μm. (c) Knocking down Stac3 in 48 hpf embryos significantly increases the proportion of progeny from a cross between $stac3^{mi34}$ heterozygous carriers that are immotile or shiver and decreases those that swim in response to touch. * denotes that the percent *stac3* MO injected progeny that were immotile or shivered was greater than control MO injected progeny (respectively, $p < 0.001$ and $p < 0.01$; t test); percent *stac3* MO injected progeny that swam was less than control MO injected progeny ($p < 0.001$, t test). ** denotes that co-injection of an expression plasmid for $stac3^{wt}$ with *stac3* antisense MO decreases immotility and restores swimming in a great majority of progeny. Percent *stac3* MO + expression plasmid for $stac3^{wt}$ injected progeny that were immotile was much less than *stac3* MO alone progeny ($p < 0.001$, t test). Error bars represent standard error of the means.

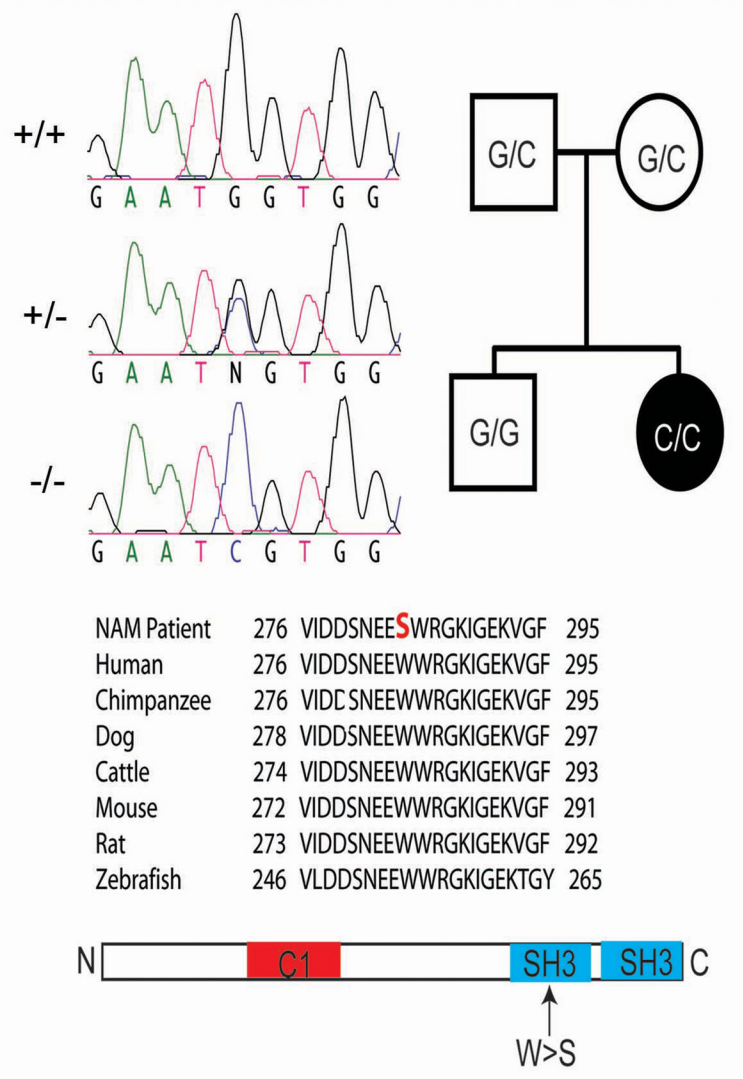

Fig. 7. Missense Mutation in Human *STAC3* causes Native American Myopathy (NAM)

Left top, sequence chromatographs of corresponding exonic region of the *STAC3* gene of individuals +/+, +/− and −/− for the NAM locus showing the G>C missense mutation in the *stac3* gene. N denotes the G/C heterozygous nucleotide. Right top, pedigree of an individual exhibiting NAM (black) and homozygous for the missense mutation (C/C). Unaffected parents were carriers for the mutation (G/C) and the unaffected sibling was homozygous for the wt nucleotide (G/G). Middle, alignment of the corresponding region of Stac3 containing NAM mutation showing that the missense mutation results in a W>S substitution in NAM individuals and that this W is completely conserved between various mammals and zebrafish. Bottom, diagram showing that the missense mutation in $Stac3^{NAM}$ is located in a SH3 domain.

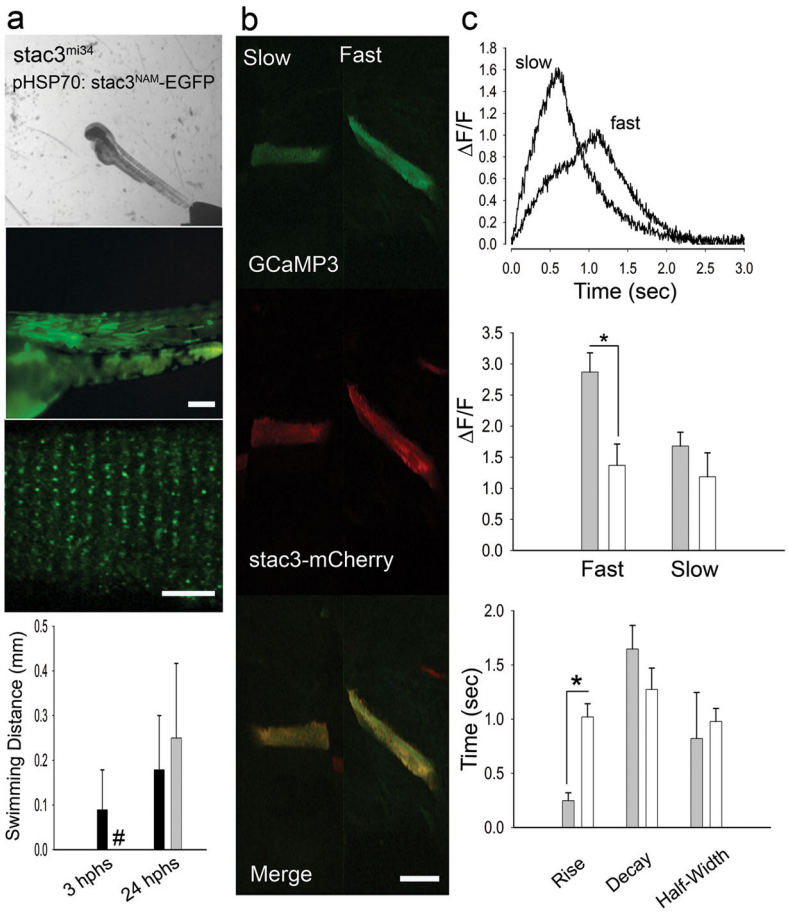

Fig. 8. The *stac3*^{NAM} Allele Decreases EC Coupling

(a) Expression of Stac3^{NAM} by muscle fibers in *stac3*^{mi34} embryos does not rescue touch evoked swimming. Superimposed frames (30 Hz) showing that a heat induced mutant embryo previously injected with *pHSP70:stac*^{NAM}*-egfp* does not swim following tactile stimulation (top) despite expression of zebrafish Stac3^{NAM}-EGFP in myotomes and triadic localization of zebrafish Stac3^{NAM}-EGFP (middle, scale bars: 180 μm and 10 μm). Histograms (bottom) quantify the comparable lack of touch evoked swimming of *stac3*^{mi34} mutants expressing the NAM allele (black) and uninjected mutants (gray) both 3 and 24 hphs. Note the difference in scale of the y axis from that in Fig. 4a that shows swimming in mutant rescued embryos. # denotes zero movement. (b) Expression of Stac3^{NAM} by muscle fibers in *stac3*^{mi34} embryos partially rescues Ca^{2+} transients *in vivo*. Left panels, examples of *stac3*^{mi34} mutant slow and fast twitch fibers co-expressing *α-actin* driven GCaMP3 and *hsp70* regulated zebrafish Stac3^{NAM}-mCherry. The triadic localization of Stac3^{wt}-mCherry cannot be seen due to the low resolution of the resonance scans used to detect the fluorescent proteins. (c) top, Ca^{2+} transients from mutant fast and slow fibers co-expressing Stac3^{NAM}-mCherry and GCaMP3. Right middle, histogram showing that peak Ca^{2+} release is decreased between mutant fast fibers expressing *stac3*^{wt} (gray, n=6) and *stac3*^{NAM} (white, n=6). Peak Ca^{2+} was not different for mutant slow twitch fibers (wt, n=2; NAM allele, n=2). Bottom, histogram showing the kinetics of Ca^{2+} transients of mutant fast fibers expressing

stac3^{wt} (gray, n=5) and *stac3*^{NAM} (white, n=9). Asterisk signifies $p<0.01$, t-test. Error bars represent standard error of the means.